

## Note: Electrical and thermal characterization of a ferroelectric thin film with an electro-thermal nanoprobe

R. Jackson, P. C. Fletcher, K. Jambunathan, A. R. Damodaran, J. N. Emmerich et al.

Citation: *Rev. Sci. Instrum.* **83**, 076105 (2012); doi: 10.1063/1.4733730

View online: <http://dx.doi.org/10.1063/1.4733730>

View Table of Contents: <http://rsi.aip.org/resource/1/RSINAK/v83/i7>

Published by the [American Institute of Physics](#).

---

### Related Articles

Variation of ferroelectric properties in (Bi,Pr)(Fe,Mn)O<sub>3</sub>/SrRuO<sub>3</sub>-Pt/CoFe<sub>2</sub>O<sub>4</sub> layered film structure by applying direct current magnetic field

*J. Appl. Phys.* **111**, 124103 (2012)

How to generate high twin densities in nano-ferroics: Thermal quench and low temperature shear

*Appl. Phys. Lett.* **100**, 222905 (2012)

Coexistence of ferroelectric vortex domains and charged domain walls in epitaxial BiFeO<sub>3</sub> film on (110)O GdScO<sub>3</sub> substrate

*J. Appl. Phys.* **111**, 104117 (2012)

Low temperature anomalous field effect in SrxBa<sub>1-x</sub>Nb<sub>2</sub>O<sub>6</sub> uniaxial relaxor ferroelectric seen via acoustic emission

*J. Appl. Phys.* **111**, 084101 (2012)

Modified electrical transport probe design for standard magnetometer

*Rev. Sci. Instrum.* **83**, 033904 (2012)

---

### Additional information on Rev. Sci. Instrum.

Journal Homepage: <http://rsi.aip.org>

Journal Information: [http://rsi.aip.org/about/about\\_the\\_journal](http://rsi.aip.org/about/about_the_journal)

Top downloads: [http://rsi.aip.org/features/most\\_downloaded](http://rsi.aip.org/features/most_downloaded)

Information for Authors: <http://rsi.aip.org/authors>

## ADVERTISEMENT



Special Topic Section:  
**PHYSICS OF CANCER**

Why cancer? Why physics? [View Articles Now](#)

## Note: Electrical and thermal characterization of a ferroelectric thin film with an electro-thermal nanoprobe

R. Jackson,<sup>1</sup> P. C. Fletcher,<sup>2</sup> K. Jambunathan,<sup>3</sup> A. R. Damodaran,<sup>3</sup> J. N. Emmerich,<sup>1</sup> H. Teng,<sup>1</sup> L. W. Martin,<sup>3</sup> W. P. King,<sup>2,3</sup> and Y. Wu<sup>1,a)</sup>

<sup>1</sup>College of Engineering, Mathematics, and Science, University of Wisconsin-Platteville, Platteville, Wisconsin 53818, USA

<sup>2</sup>Department of Mechanical Science and Engineering, University of Illinois at Urbana-Champaign, Urbana, Illinois 61801, USA

<sup>3</sup>Department of Materials Science and Engineering, University of Illinois at Urbana-Champaign, Urbana, Illinois 61801, USA

(Received 1 May 2012; accepted 21 June 2012; published online 11 July 2012)

The localized temperature-dependent piezoelectric response of ferroelectric barium strontium titanate (BST) thin films is studied using an electro-thermal (ET) nanoprobe. The ET probe provides independent electrical and thermal excitation to a nanometer-scale volume of the specimen and is capable of detecting the phase transition temperature of the BST thin films. The piezoresponse measured by the ET probe follows the temperature dependence of the piezoelectric constant, whereas with bulk heating the response follows the temperature dependence of the spontaneous polarization. The observed differences stem from the localized inhomogeneous electro-thermal field distribution at the specimen.

© 2012 American Institute of Physics. [<http://dx.doi.org/10.1063/1.4733730>]

Ferroelectric materials are extensively used in non-volatile data storage,<sup>1</sup> microscale actuators and sensors,<sup>2</sup> and microwave electronic components.<sup>3</sup> The understanding of local polarization dynamics and domain structure in ferroelectric materials has been greatly facilitated by piezoresponse force microscopy (PFM).<sup>4–8</sup> PFM is a scanning probe-based technique that detects the converse piezoelectric response of a material via bias-induced surface strains and the resulting cantilever deflection. Only a few articles consider ferroelectric response above room temperature<sup>9–12</sup> and these studies rely on atomic force microscope (AFM) compatible heater stages to control temperature. This letter describes measurements of the piezoelectric response of ferroelectric barium strontium titanate ( $\text{Ba}_{0.6}\text{Sr}_{0.4}\text{TiO}_3$ , BST) thin films around the Curie temperature using an electro-thermal (ET) nanoprobe.<sup>1</sup>

A few studies have used heated AFM probes for electrical measurements.<sup>13,14</sup> Tip-based heating provides advantages over bulk heating because the integrated heater is capable of reaching temperatures in excess of 1200 °C with thermal time constants on the order of tens of microseconds.<sup>15</sup> Tip-based heating also produces localized temperature gradients at the sample surface that can be utilized to separate local surface properties from bulk properties. The ET nanoprobe used here<sup>16</sup> facilitates independent control of electrical and thermal tip excitations.

Thin films of ferroelectric BST and amorphous silicon dioxide ( $\text{SiO}_2$ ) of 75 nm thickness were grown on an  $\text{SrRuO}_3$  buffer layer on (001)-oriented  $\text{SrTiO}_3$  single crystal substrates. The BST films were fabricated by pulsed-laser deposition. The  $\text{SiO}_2$  films were deposited via plasma-enhanced chemical vapor deposition. The  $\text{SiO}_2$  film was used as a control sample because it has a negligible piezoelectric response.

Figure 1(a) shows a scanning electron microscope micrograph of the ET probe. There are three basic elements of the probe: an integrated solid-state heater formed by two cantilever legs, a third high-doped n+ type silicon leg addressing the tip electrode, and an n-p-n semiconductor junction for electrical isolation between the heater region and the tip electrode. Figure 1(b) is a schematic diagram of the electro-thermal contact between the heated tip and the specimen, showing the relevant temperatures and the electric impedance network model of the contact. We calibrated the heater temperature using micro-Raman spectroscopy.<sup>17</sup> In the experiments, the cantilever heater temperature was varied over the range of 25 °C–553 °C. The relationship between tip-sample interface temperature,  $T_{\text{interface}}$ , and the heater temperature,  $T_{\text{heater}}$ , can be found using a previously developed thermal circuit model.<sup>18</sup> For a heated tip contacting room temperature BST in air, a maximum heater temperature of 553 °C translates to a maximum interface temperature of 219 °C for an ambient temperature,  $T_{\infty}$ , of 25 °C.

We simulated the electric and thermal field profile under the tip using the finite element program ANSYS. Simulation results show the temperature is less than 10% of its surface value and the electric field is less than 5% of its surface value beyond one tip radius from the tip into the film (see supplementary material for the details on the electro-thermal modeling).<sup>19</sup> Therefore, the piezoresponse depends on the film material within one tip radius from the tip. We refer to this volume as the signal generation volume. The signal generation volume scales with the radius of the tip, and for this study is around  $2.6 \times 10^5 \text{ nm}^3$ .

In addition to the ET probe, we also measured the piezoresponse of the BST thin film using a sample heating stage and commercial conductive AFM probes. In both local heating and bulk heating experiments, we measured the contact resonance amplitude of the cantilever under

<sup>a)</sup> Author to whom correspondence should be addressed. Electronic mail: [wuy@uwplatt.edu](mailto:wuy@uwplatt.edu).

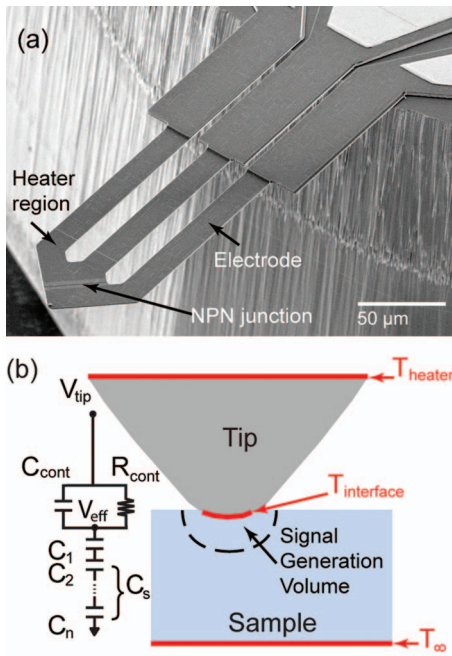


FIG. 1. (a) SEM micrograph of an electro-thermal probe showing the integrated heater, the independent electrode, and the n-p-n junction for electrical isolation. (b) Simple equivalent electric circuit model of the tip-sample contact and relevant temperatures.

fixed excitation voltage amplitude,  $V_{tip}$ , while controlling the temperature. The relation between  $V_{tip}$  and the effective voltage at the tip-sample interface,  $V_{eff}$ , is<sup>20</sup>

$$\frac{V_{eff}}{V_{tip}} = \frac{1}{\sqrt{(1 + C_s/C_{cont})^2 + R_{cont}^2 C_s^2 \omega^2}}, \quad (1)$$

where  $R_{cont}$  is the contact resistance between the tip and the sample,  $C_{cont}$  is the contact capacitance,  $C_s$  is the total capacitance of the sample, and  $\omega$  is the frequency of the oscillating electric field. Both  $C_{cont}$  and  $C_s$  are on the order of tens of attofarads at room temperature.<sup>21,22</sup>

Electrostatic coupling between the cantilever and sample can result in a spurious contribution to the measured signal in PFM.<sup>23</sup> The ET probe conducts an ac electric field to the tip while driving the integrated heater using dc. The electrostatic coupling from the dc driving voltage for different heater temperatures gives rise to flexural and torsional contact resonance modes, as shown in Figure 2. The response on the  $\text{SiO}_2$  sample is due to electrostatic coupling and it is negligible at the fundamental mode (166 kHz near room temperature) compared to the piezoresponse on the BST sample. The electrostatic coupling is dominant at the second vibration mode (185 kHz near room temperature) because electrostatic force at the geometrically off-centered heater promotes torsional modes of the three-legged cantilever.<sup>24</sup>

Figure 3(a) shows the local temperature-dependent piezoresponse at the fundamental contact resonance frequency of the ET probe on the BST and  $\text{SiO}_2$  samples. The BST piezoresponse increases, then decreases after a transition point corresponding with an interface temperature of 97 °C, whereas the  $\text{SiO}_2$  response only increases slightly with

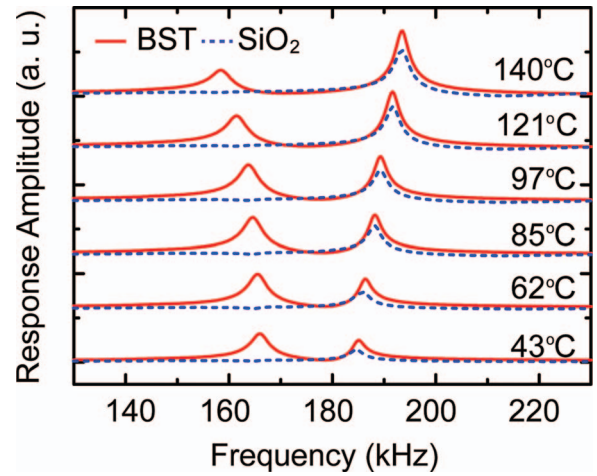


FIG. 2. Cantilever response amplitude under electric excitation for various ET probe heater temperatures. The solid red line is the response on the BST sample and the dashed blue line is the response on the  $\text{SiO}_2$  sample.

temperature due to the electrostatic effect. Figure 3(b) shows the temperature-dependent response for bulk heating. The BST response decreases monotonically until  $\sim 100$  °C, above which the response shows little change with temperature, similar to the  $\text{SiO}_2$  response for the entire temperature spectrum.

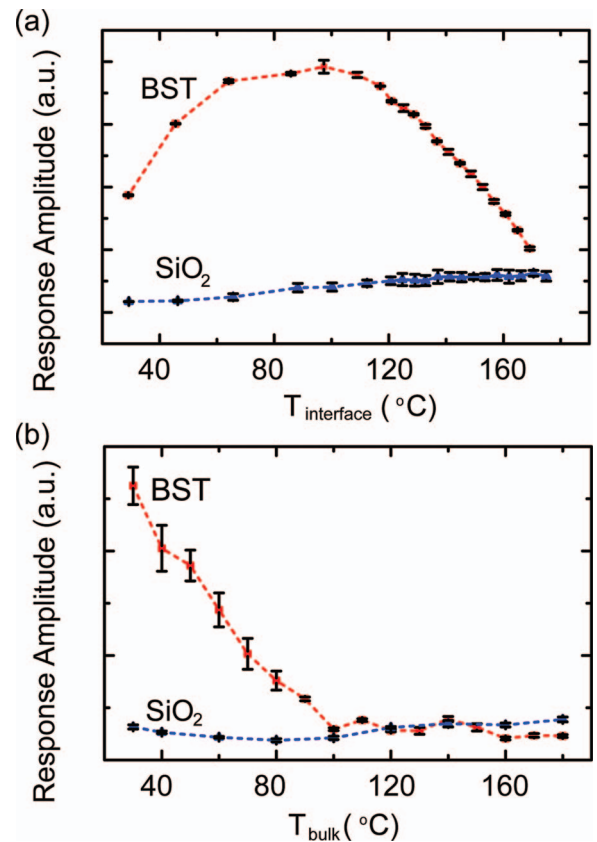


FIG. 3. (a) Contact resonance response on the BST and  $\text{SiO}_2$  samples under localized thermal and electrical excitation. The BST transition temperature corresponds to  $\sim 97$  °C. (b) Contact resonance response on the BST and  $\text{SiO}_2$  samples as a function of bulk heating temperature. The BST transition temperature corresponds to  $\sim 100$  °C.

For a homogeneously polarized, stress-free, ferroelectric material with polarization in the  $z$  direction, theoretical analysis<sup>5</sup> shows the piezoresponse signal is proportional to the electric field strength within the signal generation volume and the piezoelectric constant  $d_{33}$ . The piezoelectric coefficient  $d_{33}$  increases with temperature.<sup>25–27</sup> For bulk heating, the electric field strength decreases with increasing temperature due to the increasing dielectric constant of the BST film and thus the ratio of  $C_s/C_{cont}$  in Eq. (1). Previous published results suggested that the temperature-dependent piezoelectric response follows the spontaneous polarization when  $C_s$  is much greater than  $C_{cont}$ .<sup>11</sup> In addition, the unscreened polarization-bound charges under the cantilever also contribute to the temperature dependence of the spontaneous polarization via electrostatic coupling.<sup>9</sup> Our results using the heating stage are in agreement with results from other studies in literature using bulk heating methods.<sup>9,11</sup> The piezoresponse is observed to continuously decrease with increasing temperature, consistent with a smearing of the phase transition, as has been reported in thin film samples of ferroelectrics.<sup>28</sup> The results from the ET probe differ from those using bulk heating methods<sup>9,11</sup> and reflect the complex interplay between thermal and piezoelectric responses in the system. Our technique only heats a nanometer scale volume of material directly under the tip. The specimen away from the tip remains at room temperature, thus reducing the temperature dependent response due to the unscreened polarization-bound charges via stray capacitive coupling. The measured piezoresponse follows the temperature-dependence of  $d_{33}$ , which agrees with a recent study of the temperature-dependent piezoresponse of lead zirconate titanate using a micro-heater with minimization of the cantilever-microheater overlap region.<sup>12</sup> Furthermore, the non-uniform temperature distribution effectively limits the increase of capacitance  $C_s$  with increasing  $T_{interface}$ . With a steady electric field, the piezoresponse increases with  $T_{interface}$  until the region directly under the heated tip reaches the Curie temperature of  $\sim 100$  °C. Above the Curie temperature, the overall response decreases as a larger percentage of the signal generation volume is heated above the Curie temperature and becomes paraelectric with no piezoelectric response.

In summary, we measured the temperature-dependent piezoresponse of a ferroelectric thin film with nanometer-scale electrical and thermal excitation using an electro-thermal nanoprobe. The measured piezoresponse under localized heating differs from results using a bulk heating approach because of the localized non-uniform temperature distribution in the specimen. This study demonstrates an application of the ET nanoprobe in nanoscale electro-thermal characterization.

This work was supported by the National Science Foundation (NSF) under Grant No. 0960232. J.K. and L.W.M. acknowledge support from the Office of Naval Research (ONR) under Grant No. N00014-10-10525. A.R.D. and L.W.M. acknowledge support from the (U.S.) Army Research Office (USARO) under Grant No. W911NF-10-1-0482. The authors thank Dr. Scott MacLaren at FSMRL Central Facilities for his assistance with part of the AFM work.

- <sup>1</sup>J. F. Scott, *Science* **315**, 954 (2007).
- <sup>2</sup>N. Setter, D. Damjanovic, L. Eng, G. Fox, S. Gevorgian, S. Hong, A. Kingon, H. Kohlstedt, N. Y. Park, G. B. Stephenson, I. Stolitchnov, A. K. Taganstev, D. V. Taylor, T. Yamada, and S. Streiffer, *J. Appl. Phys.* **100**, 051606 (2006).
- <sup>3</sup>M. J. Lancaster, J. Powell, and A. Porch, *Supercond. Sci. Tech.* **11**, 1323 (1998).
- <sup>4</sup>M. Abplanalp, L. M. Eng, and P. Gunter, *Appl. Phys. A: Mater. Sci. Process.* **66**, S231 (1998).
- <sup>5</sup>S. V. Kalinin, B. J. Rodriguez, S. Jesse, E. Karapetian, B. Mirman, E. A. Eliseev, and A. N. Morozovska, *Annu. Rev. Mater. Res.* **37**, 189 (2007).
- <sup>6</sup>S. V. Kalinin, *Rep. Prog. Phys.* **73**, 056502 (2010).
- <sup>7</sup>S. Jesse, H. N. Lee, and S. V. Kalinin, *Rev. Sci. Instrum.* **77**, 073702 (2006).
- <sup>8</sup>H. Y. Guo, J. B. Xu, I. H. Wilson, Z. Xie, E. Z. Luo, S. Hong, and H. Yan, *Appl. Phys. Lett.* **81**, 715 (2002).
- <sup>9</sup>E. Z. Luo, Z. Xie, J. B. Xu, I. H. Wilson, and L. H. Zhao, *Phys. Rev. B* **61**, 203 (2000).
- <sup>10</sup>X. K. Orlik, V. Likodimos, L. Pardi, M. Labardi, and M. Allegrini, *Appl. Phys. Lett.* **76**, 1321 (2000).
- <sup>11</sup>S. V. Kalinin and D. A. Bonnell, *Appl. Phys. Lett.* **78**, 1116 (2001).
- <sup>12</sup>B. Bhatia, J. Karthik, D. G. Cahill, L. W. Martin, and W. P. King, *Appl. Phys. Lett.* **99**, 173103 (2011).
- <sup>13</sup>J. L. Remmert, Y. Wu, J. C. Lee, M. A. Shannon, and W. P. King, *Appl. Phys. Lett.* **91**, 143111 (2007).
- <sup>14</sup>J. Lee, A. Liao, E. Pop, and W. P. King, *Nano Lett.* **9**, 1356 (2009).
- <sup>15</sup>J. Lee, T. Beechem, T. L. Wright, B. A. Nelson, S. Graham, and W. P. King, *J. Microelectromech. Syst.* **15**, 1644 (2006).
- <sup>16</sup>P. C. Fletcher, B. S. Bhatia, Y. Wu, M. A. Shannon, and W. P. King, *J. Microelectromech. Syst.* **20**, 644 (2011).
- <sup>17</sup>B. A. Nelson and W. P. King, *Sens. Actuators, A* **140**, 51 (2007).
- <sup>18</sup>B. A. Nelson and W. P. King, *Nanoscale Microscale Thermophys. Eng.* **12**, 98 (2008).
- <sup>19</sup>See supplementary material at <http://dx.doi.org/10.1063/1.4733730> for finite element simulation of local electrical field and thermal field distribution.
- <sup>20</sup>R. O'Hayre, G. Feng, W. D. Nix, and F. B. Prinz, *J. Appl. Phys.* **96**, 3540 (2004).
- <sup>21</sup>D. T. Lee, J. P. Pelz, and B. Bharat, *Nanotechnology* **17**, 1484 (2006).
- <sup>22</sup>L. Fumagalli, G. Ferrari, M. Sampietro, I. Casuso, E. Martinez, J. Samitier, and G. Gomila, *Nanotechnology* **17**, 4581 (2006).
- <sup>23</sup>B. J. Rodriguez, S. Jesse, A. P. Baddorf, and S. V. Kalinin, *Phys. Rev. Lett.* **96**, 237602 (2006).
- <sup>24</sup>O. Sahin, S. Magonov, C. Su, C. F. Quate, and O. Solgaard, *Nat. Nanotechnol.* **2**, 507 (2007).
- <sup>25</sup>M. E. Lines and A. M. Glass, *Principles and Applications of Ferroelectrics and Related Materials* (Clarendon, Oxford, 1977).
- <sup>26</sup>X. Zeng and R. E. Cohen, *Appl. Phys. Lett.* **99**, 142902 (2011).
- <sup>27</sup>D. Damjanovic, F. Brem, and N. Setter, *Appl. Phys. Lett.* **80**, 652 (2002).
- <sup>28</sup>T. M. Shaw, S. Trolier-McKinstry, and P. C. McIntyre, *Annu. Rev. Mater. Sci.* **30**, 263 (2000).